

# Simultaneous PIV and Shadowgraphy Measurements in Slug Flow in Newtonian and Non-Newtonian Liquids

S. Nogueira<sup>o\*</sup>, R. Sousa<sup>o\*</sup>, J. B. L. M. Campos<sup>\*</sup>, A. M. F. R. Pinto<sup>\*</sup>, M. L.

Riethmuller<sup>o</sup>

<sup>o</sup> von Karman Institute for Fluid Dynamics  
Chaussée de Waterloo, 72  
B-1640 Rhode Saint Genèse – Belgium  
E-mail: riethmuller@vki.ac.be

\*Centro de Estudos de Fenómenos de Transporte  
Departamento de Engenharia Química  
Faculdade de Engenharia da Universidade do Porto  
4099 Porto Codex – Portugal  
E-mail: apinto@fe.up.pt

## ABSTRACT

A recent technique for performing simultaneous Particle Image Velocimetry and Shadowgraphy applied for the first time to slug flow, is presented in this work. The unsteadiness of slug flow creates the need of recording the shadow of the Taylor bubbles at the precise instant and position of the PIV measurements. Therefore, this experimental technique is used in order to characterise simultaneously the flow in the liquid and the shape of a single gas slug (Taylor bubble) rising through a vertical column of stagnant liquid using only one CCD camera. The experimental facility and technique are described and the details of the synchronisation between the two techniques are also explained. This new method is based on the fact that the PIV particles and the shadow of the bubbles can illuminate the CCD camera sensor at different gray levels. The PIV images are obtained by seeding the flow with fluorescent seeding and placing an optical filter in front of the camera so that the intense laser reflections in the interface are avoided and only the PIV particles reach the CCD sensor. The shadowgraph images are obtained by backward illumination with a board of LEDs emitting light in a wavelength that passes through the optical filter. The processing of the images is explained. The reason for keeping recording images with 8 bits is discussed. During the post-processing it is possible to combine the shadowgraph results with the velocity field acquired with PIV, therefore, solving some of the basic processing errors, which appear at the interfaces. Some limitations of the technique itself, due to the highly 3D shape of the rear of the bubbles are also discussed. The flow around a gas slug rising through a vertical column filled with a non-Newtonian fluid is also presented. These are the first quantitative measurements in slug flow for non-Newtonian flows, as long as the authors are aware.

## 1. INTRODUCTION

Slug flows are two-phase flows characterised by long bullet-shaped bubbles that almost occupy the entire cross-section of the pipe. Between the gas slug and the pipe wall flows a thin film of liquid. The rear of the gas slug is a separated region, the wake, characterised by strong mixing, where all transfer processes are enhanced.

In daily life, this type of flow is encountered, e. g., in a drinking straw that is being emptied too rapidly. Slug flow is encountered in many industrial applications, for example in the production and transportation of hydrocarbons in pipelines, in nuclear reactors during emergency core cooling, in boilers and condensers.

Several authors have already investigated slug flow and developed some models (Davies and Taylor (1950), Fernandes (1983), Barnea and Taitel (1993), etc), however there is still work to develop in the quantitative characterisation of the flow around the Taylor bubble and that is one of the objectives of the present work which follows previous researches (Nogueira *et al* (2000, 2001)). The validation of the models depends on these results. Most of the research efforts on slug flow have assumed that the liquid phase exhibits a Newtonian behaviour. However, when data and models are applied to situations where at least one of the phases is non-Newtonian, many uncertainties are present. The bubble motion behaviour in non-Newtonian fluids is of key importance in such diverse fluids as bubble columns, fermentation, polymer devolatilization and air-lift reactors. The complex viscosity of the continuous phase results in a completely different flow behaviour from that in classical Newtonian fluids. There is, therefore the need of extending the slug flow research towards non-Newtonian liquids, as it is done in this work.

Under some conditions two or more gas slugs can undergo coalescence resulting in a longer gas slug and changing drastically the flow. This phenomenon can generate several problems in industry and it is known to be dependent on the effect felt on the trailing bubble by the passage of the leading one. Therefore, in order to understand the mechanism of coalescence, the knowledge of the flow field in the wake of the Taylor bubble becomes essential (Moïssis and Griffith (1962). Three different types of wake have already been observed (laminar, transitional and turbulent) by Campos and Guedes de Carvalho (1988). Following this systematisation, PIV measurements have been performed in the wake of Taylor bubbles and the three types have been quantitatively described by Nogueira *et al* (2001). However, as was demonstrated by Nogueira *et al* (2000), when measuring the velocity in the liquid film surrounding the gas slugs it is not possible to determine the position of the interface from the PIV images. Indeed, These authors described and explained important optical effects that occur in the interface of Taylor bubbles while performing PIV measurements. The conclusion of that study was that there is the need of using a shadowgraphy technique when determining interface positions. The shadowgraphy technique has been successfully applied to determine the Taylor bubble shape and also the thickness of the falling film around it and these measurements have been essential in the characterisation of slug flow for steady and axisymmetric conditions.

For undeveloped or transient slug flow (when the bubbles are interacting between them) the bubbles are neither axisymmetric nor steady and it is necessary to record the shadow of the bubble at the precise instant and position of the PIV image. Still, not a single study has captured the behaviour of the gas and liquid phases simultaneously in slug flow and in this work a new technique proposed by Lindken and Merzkirch (2001) will be implemented into slug flow.

## 2. EXPERIMENTAL FACILITY AND MEASUREMENT TECHNIQUE

### **2.1. EXPERIMENTAL FACILITY**

The experimental investigation consists in the study of a single gas slug rising in a vertical column of stagnant liquid and liquid moving in the pipe. The experimental facility is schematised in Fig.1.

The experiments are performed in a transparent acrylic column of 6 m height and 0.032 m internal diameter. The gas bubbles are injected at the bottom of the test column. The box surrounding the test section (0.5 m × 0.12 m × 0.11 m) is filled with the studied liquid in order to minimise the optical distortion. This facility has been already extensively described (Nogueira *et al.* (2000, 2001)).

The test liquids are aqueous glycerol solutions ( $110 \times 10^{-3} \text{ Nsm}^{-2}$ ) and non-Newtonian liquids (aqueous solutions of carboxy-methyl-cellulose (CMC)).

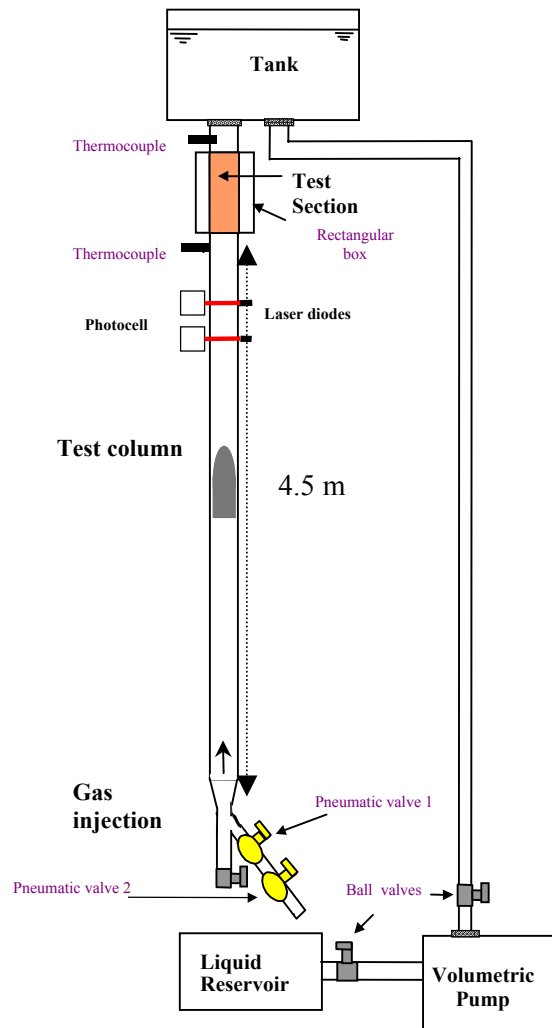


Figure 1. Experimental facility

## 2.2. SIMULTANEOUS PIV AND SHADOWGRAPHY

A new technique, recently presented by Lindken and Merzkirch (2001) for bubbly flow measurements is applied to slug flow in this work. It consists in a combination of simultaneous PIV and shadowgraphy measurements performed with the same camera. When performing PIV measurements in two-phase flow it is already a common practice to use fluorescent seeding and avoid that the intense laser reflections created at the interfaces reach the camera, by placing an optical filter in front of the camera. Like that, the only light reaching the camera has the wavelength allowed by the optical filter. This new technique is based on the fact that the PIV particles and the shadow of the bubbles can illuminate the CCD camera sensor at different gray levels. Following the previous considerations it is obvious that it is necessary to use a light source matching the PIV particles and the optical filter. Afterwards, the intensity of the background illumination has to be settled so that the PIV particles and the shadow gray levels can be differentiated.

Figure 2 shows the grey levels along the images at the marked lines, with and without bubble. It can be seen that the bubble shadow decreases the grey level of the figure in a distinct way. The processing consists in applying a median filter to the image in order to suppress the PIV particles, determining the bubble contour, for instance, by applying a derivation to the image and detecting the zeros of that function.

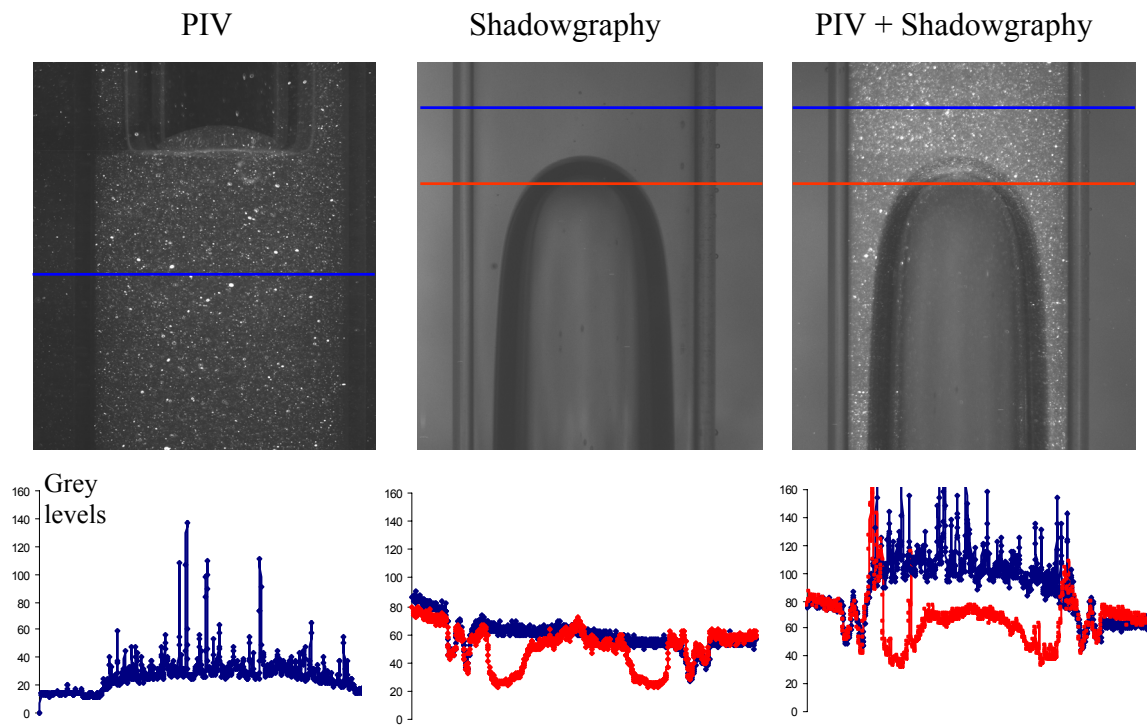


Figure 2. Principle of the technique, the PIV particles create white points with high grey level value, while the bubble contour creates a dark image with lower grey values.

### **2.3. IMPLEMENTATION OF THE TECHNIQUE FOR SLUG FLOW STUDIES**

In this work a similar technique to the one presented by Lindken and Merzkirch (2001) is implemented to slug flow. Figures 3 and 4 show, in detail, the technical apparatus used in the measurements.

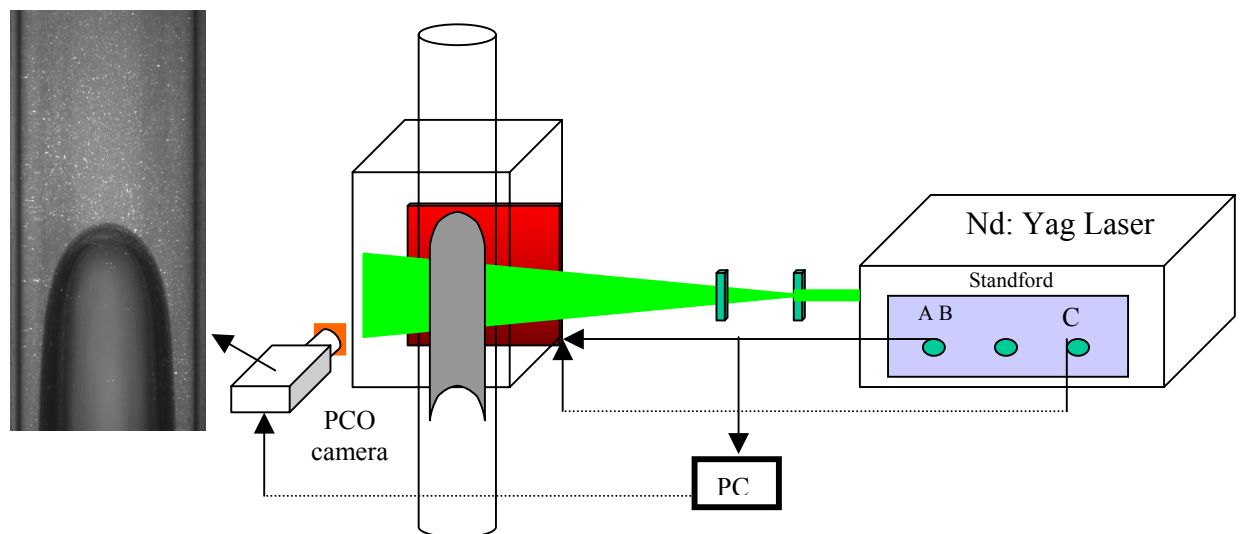


Figure 3. Detail of the facility in the test section

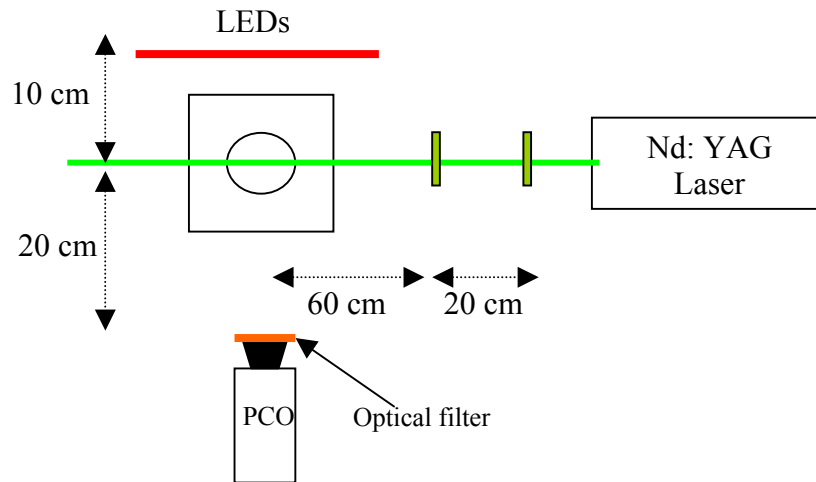


Figure 4. Upper view of the test section

The PIV images are obtained seeding the liquid with fluorescent particles and illuminating it with a double cavity pulsed Nd: Yag laser (20-400 mJ), BMI Series 5000, with a wavelength of 532 nm and pulse duration of 2.4 ns. The laser beam is formed into a laser sheet of about 1 mm thickness in the test section. A PCO (SensiCam) CCD camera, with a resolution of 1280 (H)  $\times$  1024 (V) pixels and 4096 grey levels, acquires images from an angle of 90° with the laser sheet. A red filter (model OG-570, from Image Optics components LTD), opaque below 550 nm, is used to block the intense green reflections and allows the passage of the light emitted by the fluorescent particles (around 590 nm). Therefore, the CCD chip detects only the light from the fluorescent particles. An objective of 50 mm and an extension ring of 12 mm are used to get a close view of around 4 cm  $\times$  3 cm and to get the detail of the liquid film. For measurements of the entire pipe diameter an objective of 35 mm is used. This technique and the details have already been described (Nogueira *et al.* (2000, 2001)).

The shadowgraphy images are obtained by illuminating the flow from the back with a double-pulsed light emitting diodes (LEDs) array. The LEDs emit light at 650 nm and the Taylor bubbles produce a shadow, at that wavelength, that passes through the optical filter and reaches the camera.

Tests were performed with a single LED in order to implement the LEDs system in the slug facility. The LEDs have to work in a pulsed mode and the time response after receiving the trigger has been settled to a minimum value of few nanoseconds. The duration of the pulses has also to be small enough in order to acquire a perfect defined shape of the bubble instead of a blurred image. According to this a board of 0.25 m  $\times$  0.30 m with 350 LEDs (0.003 m of diameter) has been built. Since a uniform background illumination is essential, diffuser paper has to be placed between the LEDs and the test section and care has to be taken to ensure that the LEDs are distributed uniformly in the board. An electrical system has been designed that allows the triggering of the system and pulse duration of around 12  $\mu$ s, which corresponds to a maximum displacement of 0.04 pixel of the bubble during the acquisition.

The synchronisation between the camera, laser and LEDs is done in such a way that the pulses of the laser are recorded in the same frame of the CCD camera simultaneously with the pulses of the LEDs. The signal from the Stanford signal generator works as the master and it feeds both the camera and the LEDs. The signal AB (Fig. 5) of the Stanford controls the opening of the first image of the PCO camera (the duration of the opening is the duration of the pulse), creates the pulsing of the LEDs array at the rising edge of the signal (there is a characteristic time delay of 5 $\mu$ s of the LEDs) and fires the first cavity of the laser (at the following edge of the signal). Figure 5 shows a time diagram of the synchronisation procedure. The camera opens again after a dead time of 1 $\mu$ s and grabs the images of the pulse (controlled by signal CD) of the second cavity of the laser, as well as the image of the LEDs array pulsing again (controlled by the signal C of the Stanford). Obviously the system can be adjusted in such a way that the laser and the LEDs pulses could be simultaneous, but in the present work it is

not necessary since the time difference corresponds to a displacement of 2 pixels of the bubble, for the worst case.

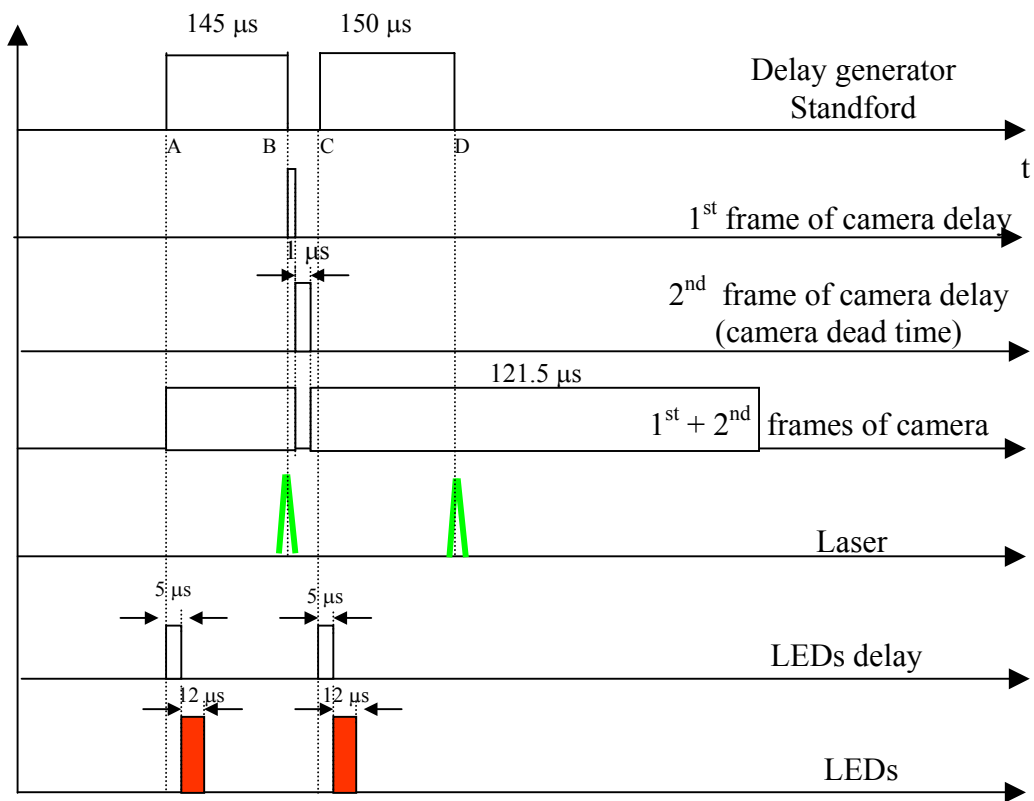


Figure 5. Time diagram of the synchronization between the LEDs, laser and camera

#### 2.4. IMAGE PROCESSING

The images acquired with this technique contain both the PIV (flow field) and shadowgraphy (bubble shape) information. The processing is made separately.

The processing of the image to obtain the shadow of the Taylor bubble is performed in several steps. Figure 6 shows an example of an image acquired with simultaneous PIV and shadowgraphy.



Figure 6. Simultaneous PIV and shadowgraphy image of a Taylor bubble (gas slug)

Figure 6 shows a final image in which the intensity of the LEDs is adjusted but it is important to refer to the importance of the uniformity of the image, as well as to avoid shadows in the liquid film around the Taylor bubble. The PIV particles in the flow create a highly noisy graphic of the grey levels of the bubbles. Therefore, a median filter is applied to the original image and the result shown in Figure 7a shows an image with more uniform background.

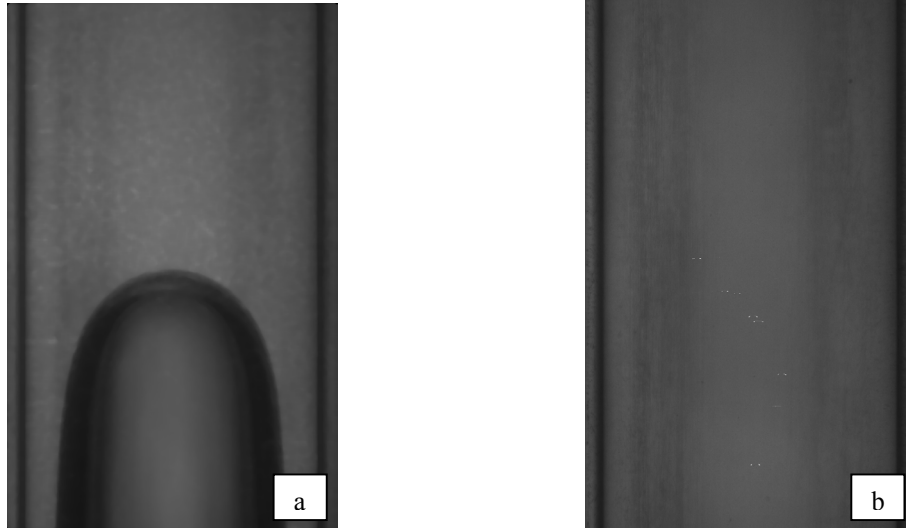


Figure 7. a) Image of the bubble after applying a median filter; b) image of the background illumination

Unlike the method used by Lindken and Merzkirch (2001), in which the bubbles interfaces were determined by the derivative of the gray level applying a filter, the gas slug shadow is extracted by subtracting this image (Fig. 7 a) to a reference image with the background illumination (Fig. 7 b). The resulting image of this operation is represented in the next figure.

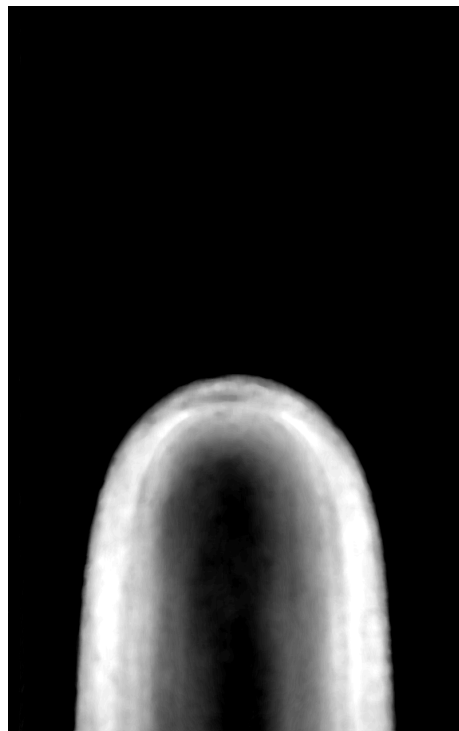


Figure 8. Image resulting from the subtraction between the image after the median filter and the background image.

The complete shadow of the bubble is obtained after binarization of image in Fig. 8 with a selected threshold (Fig. 9 a). Figure 9 b shows the image of the bubble after filling the center of the bubble. The filling of the bubble is not essential to determine the bubble shape but can be of advantage when post-processing PIV results since it can be used to eliminate wrong vectors that appear inside the bubbles.

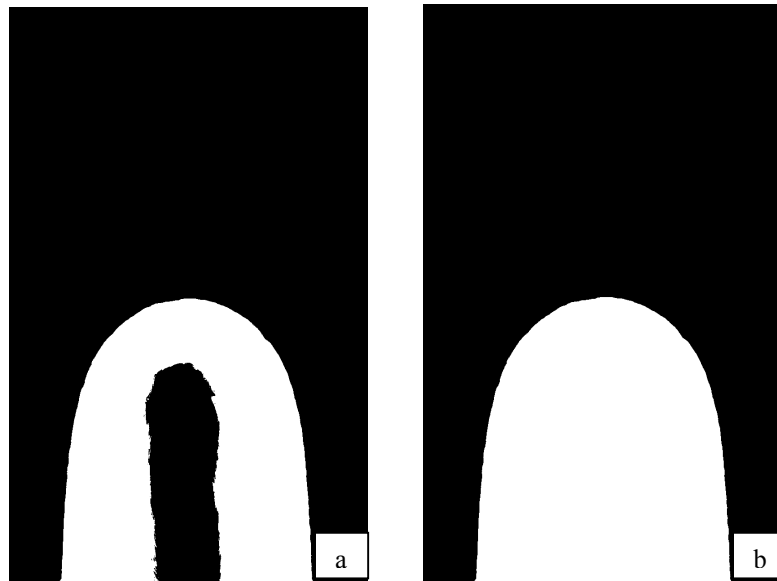


Figure 9. Final shape of the Taylor bubble; a) shadow resulting from binarisation, b) shadow after filling the center of the bubble

An advantage of processing the images by subtracting a reference image with the background illumination is that, like this, only the bubble shape is obtained, while when processing performing the derivative of the image gray level also the Plexiglass column is retrieved and has to be eliminated.

The digital PIV images are processed separately using the cross-correlation algorithm WIDIM, developed at VKI by Scarano and Riethmuller (1999, 2000). In this process, the interrogation windows are displaced and their size is reduced iteratively. The processing of the PIV images uses a three point-fit for the sub-pixel interpolation peak determination. The time interval between two successive images is reduced to avoid loss of pairs due to 3D motion in the wake of the bubbles and varies from  $600 \mu\text{s}$  to 2 ms. For measurements in the liquid film this time changes from  $200 \mu\text{s}$  to  $800 \mu\text{s}$ . The initial image has  $1280 \text{ (H)} \times 1024 \text{ (V)}$  pixels and the initial window size is of  $64 \times 32$  pixels, according to the privileged flow direction. The number of refinement steps and, therefore, the size of the final window and the number of vectors determined, depend on the different measurements areas and velocities. It is largely accepted that the mainly uncertainty associated with PIV measurements is less than a tenth of a pixel. The high resolution allowed by the PCO camera leads to an estimated uncertainty of 1.5%.

### 3. RESULTS AND DISCUSSION

Figure 10 shows two consecutive images of a Taylor bubble rising in a viscous aqueous solution of glycerin. The first image (a) corresponds to normal PIV, no backward illumination is used, while image (b) has been obtained by illuminating the test section simultaneously with the LEDs and the laser sheet. It is evident in Fig 10a that PIV particles are seen inside the bubble. Figure 10b gives the exact position of the bubble interface and confirms that the particles are inside the bubble and are only observed due to optical distortion. This is the *mirage effect* referred by Nogueira *et al* (2000), which means that the same pair of particles appears 3 times in the image: the real particle image, its reflection at the bubble's interface and the refracted image inside the bubble.

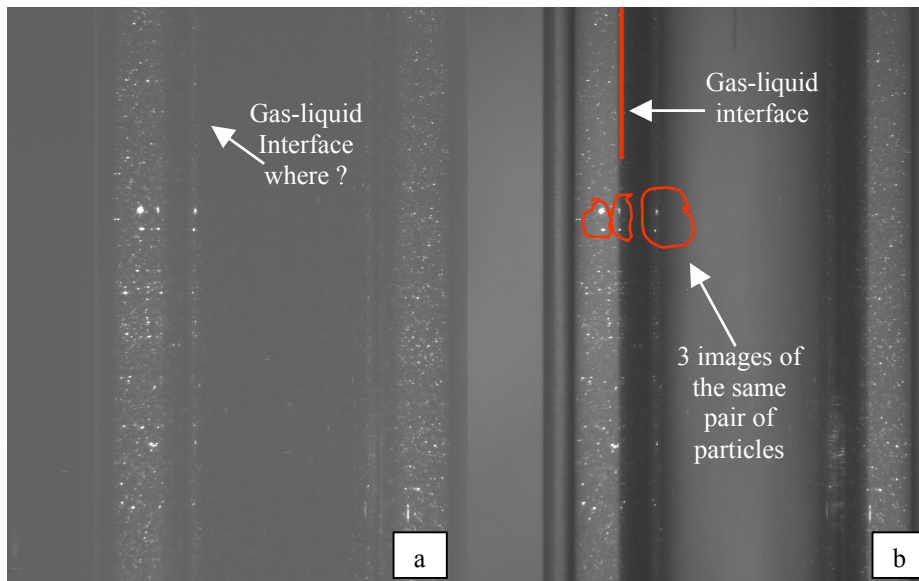


Figure 10. PIV image of a Taylor bubble without (a) and with (b) LEDs background illumination

The images are recorded with 8 bits, which gives 256 levels of grey although the PCO camera used allows the acquisition with 12 bits and therefore, 4096 levels of grey. Indeed, 8 bits images already give sufficiently accurate gas-liquid interface positions as it can be seen in the clear drop of the grey level in Fig. 2. Concerning the flow field, acquiring 8 bits images instead of 12 bits does not affect the correlation robustness, as was pointed out by Gouriet *et al* (2001).

Figure 11 shows three successive images taken of the rear of a Taylor bubble rising in a solution of CMC 0,1 % (w/w), with apparent viscosity of around  $7 \times 10^{-3} \text{ Nsm}^{-2}$ . The unsteadiness of the rear of the bubble is evident. The shape of the rear of the bubble changes from image to image. It can also be seen that the rear of the bubble has a three dimensional shape. This shape can never be completely recovered by the use of a shadow image, which only retrieves the projection of the 3-D shape in a 2-D plane and this is a limitation of the present technique. Another limitation of the technique appears when there are reflections of PIV particles at the rear of the bubbles for certain geometries, as it can be seen in the first image of Fig. 11. Here the shape of the bubble determined after the processing presented in Fig. 12 is not the exact one. Moreover it is not possible to say if the shapes that are determined, even when they retrieve the exact form of the bubble are at the center of the pipe, where the PIV measurements are performed. Attention has to be taken when analyzing the results.

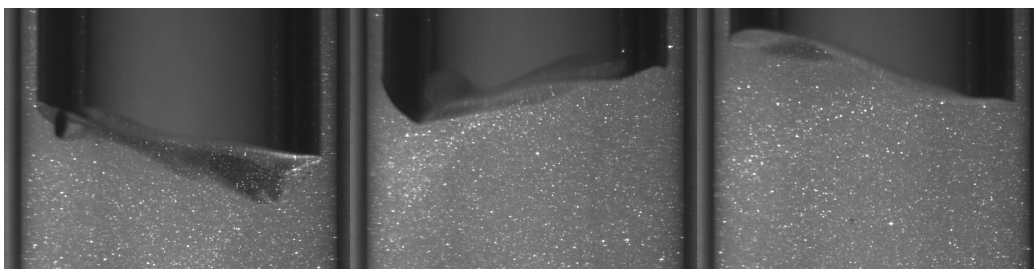


Figure 11. Consecutive images of the rear of a Taylor bubble rising in a solution of CMC 0.6% (w/w).



Figure 12. Shape of the rear of the Taylor bubble shown in Fig. 11 obtained after the processing.

There is the idea than when applying these two techniques simultaneously, the PIV images that will appear in the final image will mean that the laser sheet is in front of the bubble and there is a common believe that if the laser sheet is behind the bubble then the image will only show the shadow. Therefore, one could say, looking at Fig. 11 that the PIV particles illuminated by the laser sheet are apparently in front of the bubble rear. But, looking at Fig. 13, one can see PIV particles that are inside the spherical cap below the Taylor bubble, which means it is possible to see PIV particles even behind part of the bubble. Of course, it is a small part of the bubble and it is not the same case as Fig. 12, but still the question of determining where the border lies stay. The issue is that it is still impossible to be completely sure about the shape of highly 3-D bubbles with this technique.

Figure 13 shows a complete image of simultaneous PIV and shadowgraph of a Taylor bubble rising in a solution of CMC 0.6 % (w/w), with viscosity varying from  $100 \times 10^{-3}$  to  $300 \times 10^{-3}$  Nsm<sup>2</sup>, together with its magnification close to the rear of the bubble. The flow field obtained from this image is presented in Figs. 14 a and 14 b. The liquid film entering in the wake can be observed. As expected the velocity in the liquid film increases at it approaches the bubble interface, satisfying the full-slip condition in the gas-liquid interface.

The PIV algorithm WIDIM process the entire image, thus, creating velocity vectors in the entire field, unless that a mask is used. Masks are normally created for walls for which the interface position is known as well as the velocity, which has to verify the non-slip condition. In the case of two-phase flow a mask with a known velocity can not be use because the position and the velocity of the interface are not known. The new technique allows the determination of the exact position of the gas-liquid interface. Fig. 14b shows that after having the exact Taylor bubble coordinates it is possible to eliminate the wrong vectors that were calculated at the interior of the bubble from the PIV images.

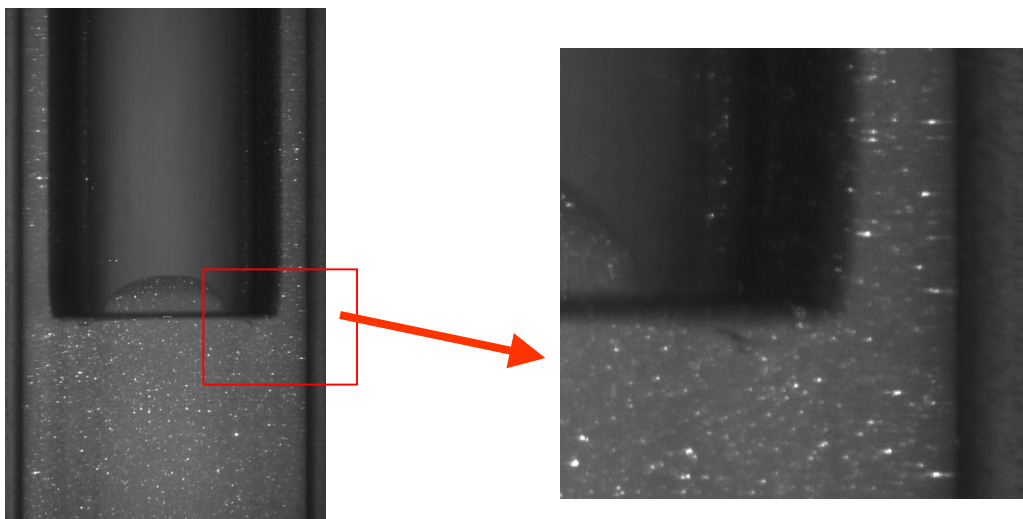


Figure 13. Simultaneous PIV and shadowgraphy images of a Taylor bubble rising in a solution of CMC 0.6 % (w/w).

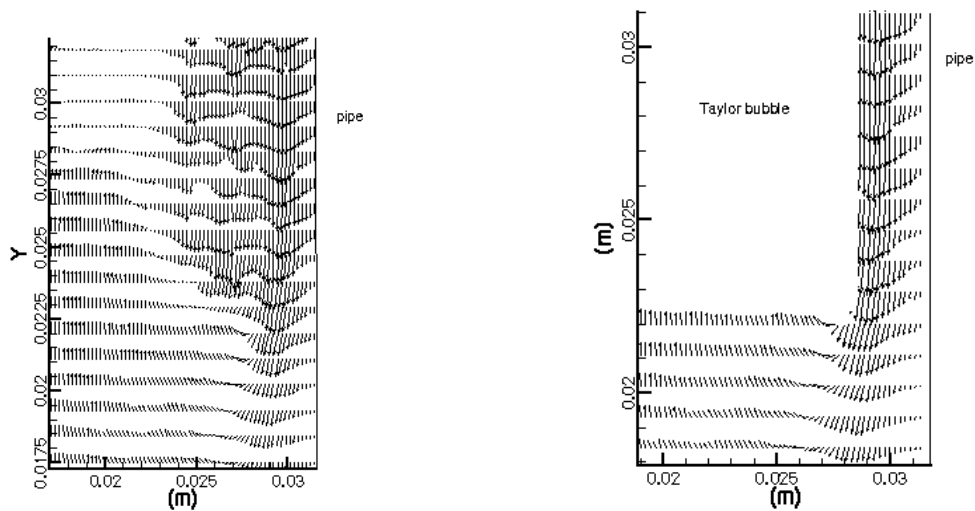


Figure 14. Flow field at the rear of a Taylor bubble rising in a solution of CMC 0.6 % (w/w).

#### 4. CONCLUSIONS

In the present work a new technique that allows simultaneous determination of Taylor bubble's shape and flow field around it is successfully applied. The use of this technique is essential due to the unsteady behavior of slug flow under certain conditions. The shape of the bubbles is determined using background illumination provided by a board of 350 LEDs, while the flow field in the liquid is determined applying fluorescent PIV technique. The synchronization between the two techniques is done using a delay generator Stanford.

The images are acquired in 8 bits because there is not a clear advantage in recording with 12 bits. The level of grey of the images are optimized by settling the LEDs' intensity so that the processing retrieves the accurate shape of the bubble.

The three-dimensional features of the flow create limitations in the determination of the bubble shape because the shadowgraphy technique retrieves only the two-dimensional shape of the bubble, which is the projection of the shadow of the bubble across the pipe. Moreover, reflections and images of PIV particles inside the bubble can lead to incorrect bubble's shape. It is still not possible to determine the shape of the Taylor bubble at exactly the center of the pipe, to be able to use the results together with the flow field from the PIV. These limitations of the technique presented are discussed and have to be taken into account while analyzing results.

The simultaneous PIV and shadowgraphy technique allows the determination of the exact position of the gas-liquid interface at the moment of the PIV measurements. Therefore, the flow field around the Taylor bubble can be corrected by eliminating the wrong vectors processed inside the bubble.

#### REFERENCES

- Lindken, R. and Merzkirch, W. (2001), "A novel PIV technique for measurements in multi-phase flows and its application to two-phase bubbly flows", 4<sup>th</sup> International Symposium on Particle Image Velocimetry, Gottingen, Germany, September 17–19, 2001.
- Davies, R. M. and Taylor, G. I. (1950), "The mechanism of large bubbles rising through extended liquids and through liquids in tubes", *Proc. R. Soc. London A*: 375-90.
- Fernandes, R. C., Semiat, R. and Duckler, A. E. (1983), "A hydrodynamic model for gas-liquid slug flow in vertical tubes", *AICHEJ*, 29, pp. 981-989.
- Barnea, D. and Taitel, Y. (1993), "A model for slug length distribution in gas-liquid slug flow", *Int. J. Multiphase Flow*, 19, pp. 829-838.

- Nogueira, S., Dias, I., Pinto, A. M. F. R. and Riethmuller, M. L. (2000), "Liquid PIV measurements around a single gas slug rising through stagnant liquid in vertical pipes", Bound Volume of Selected Papers of the "10<sup>th</sup> Symposium on Laser techniques applied to Fluid Dynamics", *Springer – Verlag*.
- Nogueira, S., Riethmuller, M. L., Campos, J. B. L. M. and Pinto, A. M. F. R. (2001), "Flow patterns in the wake of Taylor bubbles rising in stagnant liquid: an experimental study", 4<sup>th</sup> International Conference in Multiphase Flow, New Orleans, 27 May – 1 June.
- Moissis, R. and Griffith, P. (1962), "Entrance effects in a two-phase slug flow", *J. Heat Transfer*, 84, pp.29-39.
- Campos, J. B. L. M. and Guedes de Carvalho, J. R. F. (1988), "An experimental study of the wake of gas slugs rising in liquids", *J. Fluid Mechanics*, 196, pp.27-37.
- Scarano, F. and Riethmuller, M. L. (1999), "Iterative multigrid approach in PIV image processing with discrete window offset", *Exp Fluids*, 26, pp.513-523.
- Scarano, F. and Riethmuller, M.L. (2000), "Advances in iterative multigrid PIV image processing", *Exp. Fluids*, 29, pp.S051-S060.
- Gouriet, J.-B., Stitou, A. and Riethmuller, M. L. (2001), "Practical implications of camera resolution and peak locking in actual measurements", 4<sup>th</sup> International Symposium on Particle Image Velocimetry, Gottingen, Germany, September 17 –19.